Removal of arsenate from water by using an Fe–Ce oxide adsorbent: Effects of coexistent fluoride and phosphate

Yu Zhang [a,*], Xiao-Min Dou [a,c], Min Yang [a,*], Hong He [a], Chang-Yong Jing [a], Zi-Yu Wu [b]

[a] State Key Laboratory of Environmental Aquatic Chemistry, Research Center for Eco-Environmental Sciences, Chinese Academy of Sciences, P.O. Box 2871, Beijing 100085, China
[b] Beijing Synchrotron Radiation Facility, Institute of High Energy Physics, Chinese Academy of Sciences, Beijing 100049, China
[c] College of Environmental Science & Engineering, Beijing Forestry University, Beijing, 100083, China

ARTICLE INFO

ABSTRACT

The Langmuir two-site equation, X-ray photoelectron spectroscopy, and extended X-ray absorption fine structure spectroscopy have been employed to study the competitive behaviors of fluoride (F) and phosphate (P) in relation to arsenate adsorption on an Fe–Ce adsorbent as well as the mechanisms involved. The two-site isotherm revealed the presence of two kinds of adsorption sites with different binding affinities for arsenate. Both the total and low-binding-energy maximum adsorption capacities (Q and Q_1) of arsenate decreased significantly even at a molar ratio of As/P = 1:0.1. The coexistence of F, only influenced the total Q of arsenate at high simultaneous F concentrations. The fact that Fe–Ce released 0.15–0.24 mmol sulfate for every mmol arsenate adsorbed suggested that, while sulfate groups might have played a role for adsorption, surface hydroxyl groups should be the major active sites. The XPS results indicated that arsenate and P are mainly adsorbed through the substitution of Fe surface active sites, while F is mainly adsorbed through substitution of Ce surface active sites. The As k-edge EXAFS data show that the second peak of Fe–Ce after arsenate adsorption is As–Fe shell, which further supported that arsenate adsorption occurs mainly at the Fe surface active sites.

© 2010 Elsevier B.V. All rights reserved.

1. Introduction

The occurrence of arsenic (As) in groundwater has become a major health issue, and adsorption techniques have been mainly used for its removal because of their low cost and high efficiency [1,2]. However, in some cases, As in groundwater co-exists with fluoride (F) or phosphate (P), which are believed to compete with As for adsorption sites on As adsorbents [3–5]. Investigation of the competitive behavior of F and P on the adsorption of As is therefore very important from the viewpoint of engineering applications. In addition, understanding the competitive adsorption mechanisms of these anions could provide insight into the reactions occurring on the surfaces of adsorbents, leading to the elucidation of adsorption mechanisms of different adsorbents. Recently, an iron–cerium (Fe–Ce) bimetal oxide adsorbent has been successfully developed for arsenate removal, which has a higher adsorption capacity (2.00 mmol g^{-1}) than many reported adsorbents [6]. Batch

and long-term column studies on arsenate adsorption performance using groundwater samples from Inner Mongolia and the suburbs of Beijing, respectively, have shown that the adsorbent is a promising one, although its performance might be affected by some coexisting substances [7,8]. However, how F or P competes with arsenate for sites on the adsorbent surface has hitherto been unclear.

The ability of phosphate to compete with arsenate in binding at the surface sites of goethite as well as soil has well been documented [9–13]. In view of the fact that similar amounts of phosphate and arsenate were adsorbed on goethite samples at pH 3.0–8.5, Liu et al. [12] speculated that these anions compete primarily for a similar set of surface sites on this mineral, while there are some sites that are specific for arsenate and phosphate adsorption, respectively. Some researchers have attempted to describe the competitive behaviors of P and arsenate on goethite and gibbsite by using a surface complexation model (SCM), but they found the actual reactions to be more complicated than those assumed in the SCM [11,14]. The above-mentioned studies were based mainly on macroscopic adsorption observations and surface complexation models. As regards the competition between arsenate and F, little information is available.

On the other hand, by assuming that adsorption occurs at both relatively high- and low-energy surface adsorption sites [15], the Langmuir two-site model has been successively used to describe

* Corresponding authors at: State Key Laboratory of Environmental Aquatic Chemistry, Research Center for Eco-Environmental Sciences, Chinese Academy of Sciences, P.O. Box 2871, Beijing 100085, China. Tel.: +86 10 6292 3475; fax: +86 10 6292 3541.
E-mail addresses: zhangyu@rcees.ac.cn (Y. Zhang), yangmin@rcees.ac.cn (M. Yang).

the adsorption of P and arsenate on soils [16–20]. Recently, the Langmuir two-site sorption isotherm has also been used to reveal the presence of two kinds of adsorption sites for orthophosphate adsorption in cationized solid wood residues and F adsorption on Fe–Al–Ce trimetal oxide [21,22], and for the study of competitive mechanisms of Pb, Cu, and Cd on peat [23].

Although the above approaches such as SCM or Langmuir two-site equation have been widely applied in describing the adsorption processes [11,14,15,17–19,20,23], some researchers considered that the surface species and parameters selected may not be unique or physically meaningful. Very little information is available on the adsorption sites involved in the competitive adsorption of anions and no direct evidence has been provided for the competitive adsorption of anions. Fortunately, recent advances in IR, X-ray photoelectron spectroscopy (XPS), and X-ray absorption spectroscopy (XAS) have permitted detailed structural and chemical observation of adsorbents and adsorbates, providing more direct evidences and quantitative information [24]. Especially the XAS analysis has been demonstrated to be a versatile structural probe for studying the local environmental conditions for the adsorption of anions.

The aim of this study was to determine the competitive behaviors of P and F on arsenate adsorption and the mechanisms by which this occurs. The Langmuir two-site isotherm was used to describe arsenate adsorption on Fe–Ce in the simultaneous presence of F or P at various anion molar ratios, and the evidences for different adsorption sites have been obtained by integrating information from XPS and extended X-ray absorption fine structure spectroscopy (EXAFS) analyses. This study will improve the understanding of the bonding mechanisms of arsenate, F, and P on the surfaces of different adsorbents, and provide useful information regarding the application of adsorbents for arsenate removal.

2. Materials and methods

2.1. Materials

All chemicals used were of analytical reagent grade. $100\,mmol\,L^{-1}$ stock solutions of arsenate, P, and F ions were prepared by dissolving dibasic sodium arsenate, potassium dihydrogen phosphate, and sodium fluoride, respectively, in distilled water. Fe–Ce bimetal oxide adsorbents were prepared by a co-precipitation method and were characterized as described in our previous work [6,7].

2.2. Adsorption experiments

Batch equilibrium adsorption experiments were performed for single (arsenate) and binary (As/P and As/F) solution by the Fe–Ce oxide. The suspension was mixed on a rotator at 120 rpm and 20 °C for 24 h at an equilibrium pH of 5.0. The solution was then filtered through a 0.45 μm membrane filter for the analysis of As, P and F. The pH was measured with a pH meter (model 828, Orion, USA). Arsenate was analyzed using a hydride generation atomic fluorescence spectrometer (HG-AFS-610, Beijing Raileigh Analytic Instrument Corporation, China). The adsorption isotherms of As were studied by varying the dose of adsorbent at a fixed initial arsenate concentration (13.3 μmol L^{-1}), which is close to its actual concentration in groundwater in some areas of Inner Mongolia [6]. For competitive adsorption of P vs. As and F vs. As, series of molar ratios of As to P (1:0.1, 1:1, and 1:10) and As to F (1:1, 1:10, and 1:100) were employed.

Batch experiments were conducted to study the possible sulfate release in the adsorption process since sulfate was introduced in the preparation of Fe–Ce bimetal oxide. The Fe–Ce solid concentration was fixed at 300 mg L^{-1} and 6 g L^{-1} respectively, and the initial

arsenate concentration ranges at low (0.27–0.53 mM) and high (5.34–13.35 mM) corresponding to the low and high solid concentration levels. pH was maintained at 5.0 ± 0.2 using HCl and NaOH. The experimental procedure was the same as arsenate adsorption, and sulfate was analyzed using an ion chromatography (model 861, Metrohm, Swiss). Control adsorption tests were also carried out in order to determine the blank adsorption. Adsorption experiments were performed in triplicate, and the results are the averages of the three experiments.

2.3. Adsorption equations

Langmuir one-site and Langmuir two-site equations [20] were used to describe the adsorption of arsenate, As/F, and As/P on the Fe–Ce adsorbent. The Langmuir one-site equation is:

$$Q_e = \frac{bQ_0C_e}{1+bC_e} \qquad (1)$$

where Q_e denotes the amount of adsorbed anions, mmol g^{-1}; C_e is the equilibrium concentration of the respective anions, mM; Q_0 is the maximum capacity of arsenate adsorption, mmol g^{-1}; and b is the adsorption equilibrium constant related to bonding energy, L mmol^{-1}.

The Langmuir two-site equation is as follows:

$$Q_e = \frac{b_1Q_1C_e}{1+b_1C_e} + \frac{b_2Q_2C_e}{1+b_2C_e} \qquad (2)$$

where Q_1 and b_1 represent the maximum adsorption capacity and adsorption equilibrium constant for the low-binding surface and Q_2 and b_2 are the corresponding values for the high-binding surface. The maximum total adsorption capacity, Q, is written as:

$$Q = Q_1 + Q_2 \qquad (3)$$

Data analysis: Fitting of the adsorption isotherms and calculation of the parameters in Eqs. (1) and (2) were undertaken by nonlinear regression using Origin 7.0. The goodness-of-fit of the Langmuir equations was compared by single regression analysis of the actual and predicted arsenate adsorptions for each sample [25].

2.4. Characterization experiments

The binding energies and atomic ratios were measured on an XPS equipped with an ESCA-Lab-5 spectrometer. The pass energy was 50 eV and a conventional Al-K_α anode radiation source was used as the excitation source. The XPS results were corrected by C1s and the calibration energy was 284.6 eV. XPS data processing and peak fitting were performed using a nonlinear least-squares fitting program (XPSPeak software 4.1, Raymund W.M. Kwok).

Transmission XAS spectra of the Fe K-edge for Fe–Ce sample was collected at beamline BL10B at Photon Factory (KEK-PF) in the High Energy Accelerator Organization (KEK-PF, Tsukuba, Japan) with a 2.5 GeV ring energy and a 300–200 mA ring current. The monochromator used was based on a Si (3 1 1) channel cut single crystal and had an energy resolution of about 1 eV. The incident and transmitted X-rays were monitored by means of N$_2$-filled ionization chambers of lengths 14 cm and 28 cm, respectively. This sample was scanned twice in 2–3 eV steps at count times of 4–6 s.

Transmission XAS spectra of As K-edge for arsenate adsorbed Fe–Ce (adsorption capacity amounts to 130 mg g^{-1} at pH 5), synthesized CeAsO$_4$ (mainly of CeAsO$_4$ and NaCeAsO$_4$ confirmed by XRD), and scorodite (FeAsO$_4$·2H$_2$O) (obtained from Chinese Geology Museum) were collected at the 4W1B beamline of the Beijing Synchrotron Radiation Facility (BSRF). The storage ring was operated at 2.2 GeV with a beam current of 80 mA. A Si(III) double crystal monochromator was used to provide an energy resolution of 1.5 eV.

Table 1
Langmuir one and two-site equation parameters calculated using nonlinear-curve-fitting for adsorption isotherms of different arsenate, As/P, and As/F systems on Fe–Ce.

System	b_1 (L mmol^{-1})	Q_1 (mmol g^{-1})	b_2 (b^a) (L mmol^{-1})	Q_2 (mmol g^{-1})	Q(Q_0^a) (mmol g^{-1})	R^2
As[a]	–	–	13,105[a]	–	1.33[a]	0.7568[a]
As	288	1.05	88,497	0.80	1.85	0.9761
As/P = 1:0.1	273	0.96	86,470	0.79	1.75	0.9579
As/P = 1:1	610	0.23	62,274	0.74	0.97	0.9870
As/P = 1:10	–	–	–	–	–	–
As/F = 1:1	82	1.15	36,533	0.65	1.80	0.9839
As/F = 1:10	123	0.80	21,171	0.58	1.38	0.9772
As/F = 1:100	46	0.62	8224	0.57	1.19	0.9940

[a] Langmuir one-site equations calculated using nonlinear-curve-fitting for adsorption isotherms of arsenate on Fe–Ce.

These samples were loaded in Teflon sample holders, which were then sealed with Kapton tape (CHR Industries).

EXAFS data reduction and analysis were performed with WinXAS 2.3 software [26]. Theoretical EXAFS simulations were performed using FEFF 7.0 [27]. The data reduction procedures were as follows: (1) two scans per sample were aligned and then averaged; (2) first- and second-order polynomial functions were used to fit the pre-edge region for background removal and the post-edge region for normalization, respectively; (3) the spectra were then converted to photoelectron wave vector (k) space with respect to E_0 determined from the second derivative of the raw spectra; (4) $\chi(k)$ spectra for Fe–Ce after arsenate adsorption and the reference samples (CeAsO$_4$ and FeAsO$_4$·2H$_2$O) were extracted using a cubic spline function consisting of ≤ 7 knots over the range $k = 3.5\,\text{Å}^{-1}$–14.7 Å^{-1}. A k^3-weighted $\chi(k)$ function was Fourier-transformed over $k = 3.5$–14.7 Å^{-1} to obtain radial structure functions (RSFs) using a Bessel window function and a smoothing parameter (β) of 3 to minimize the effects of truncation in the RSFs without any phase shift correction. For Fe–Ce, a k range of 2.4–11.7 Å^{-1} was used, and weighted by 2 in k-space and R-space; (5) the experimental spectra were fitted with single-scattering theoretical phase shift and amplitude functions calculated with the *ab initio* computer code FEFF 7 using atomic clusters generated from the crystal structure of butlerite (FeSO$_7$H$_3$) for Fe–Ce, using CeAsO$_4$ for synthesized CeAsO$_4$, and using scorodite (FeAsO$_4$•2H$_2$O) for scorodite reference sample and arsenate adsorbed sample, respectively. The many-body amplitude reduction factor (S_0^2) was fixed at 0.9. For Fe K-edge and As K-edge, each spectrum was fit roughly to estimate ΔE_0 firstly, the difference in threshold energy between theory and experiment, by fixing coordination numbers (CN) and Debye–Waller parameter (σ^2) as the same value as that of related reference model oxide (e.g. butlerite, scorodite), then ΔE_0 was fixed to the best fit. Finally, the spectrum was fitted using estimated values for CN, R, and σ^2 as starting values, fitting results were evaluated by residual value, a good fit was considered with a residual value less than 20. Error estimates of the fitted parameters were CN, ±20%; R, ±0.02 Å; and σ^2, ±20–30%.

3. Results and discussion

3.1. Adsorption behavior

3.1.1. Adsorption equilibrium isotherm of arsenate

The Langmuir one-site and two-site equations [16,20,23] were used to fit the adsorption isotherms of arsenate at a given concentration range (Figure S1, Supplementary material). As shown in Table 1, the predicted adsorption capacities (Q_0 and Q) were 1.33 mmol g^{-1} and 1.85 mmol g^{-1} for the Langmuir one-site and two-site equations, respectively. The two-site equation showed a much better fit on the basis of the correlation coefficients (R^2) of 0.9761 and 0.7568 for the two-site and one-site equation, respectively. Thus, it could exist two different arsenate adsorption sites (Q_1 and Q_2 sites) on the Fe–Ce surface, one with a low

adsorption energy (energy related adsorption equilibrium constant $b_1 = 288$ L mmol^{-1}) and the other with a high adsorption energy ($b_2 = 88497$ L mmol^{-1}). The low-energy surface site, at which arsenate is loosely bound, has a higher maximum absorption capacity ($Q_1 = 1.05$ mmol g^{-1}), while the high-energy site, at which arsenate is relatively tightly bound, has a smaller maximum absorption capacity ($Q_2 = 0.80$ mmol g^{-1}).

3.1.2. Arsenate adsorption behavior in the presence of P/F

Fig. 1(a) and (b) shows the effects of P and F, respectively, on arsenate adsorption at different molar ratios. Except for the As/P (1:10) system, other systems showed $R^2 > 0.95$ for the two-site equation (Table 1), indicating that the adsorption of As in the As/P and As/F systems obeys the two-site model on the surface of Fe–Ce over a wide range of molar ratios. With the decrease
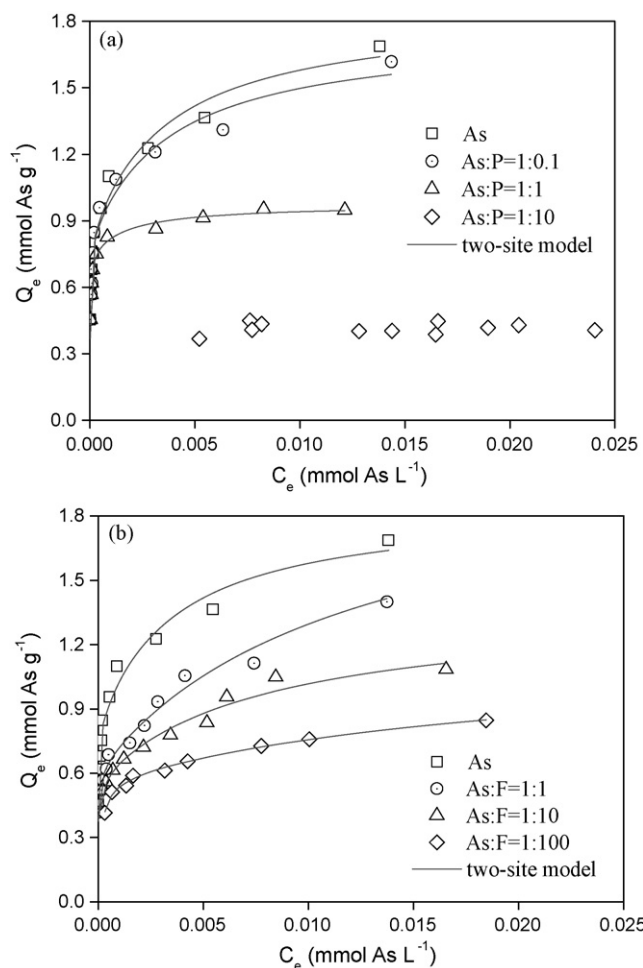

Fig. 1. Effects of (a) P and (b) F on arsenate adsorption on Fe–Ce. The solid curves are the results of the two-site Langmuir model.

of the As/P molar ratio from 1:0.1 to 1:1, the predicted arsenate adsorption capacity (Q) decreased significantly from 1.75 mmol g^{-1} to 0.97 mmol g^{-1}. The decrease in Q mainly occurred at the low-binding-energy sites (Q_1 decreased from 0.96 mmol g^{-1} to 0.23 mmol g^{-1}), while the high-binding sites seemed to be more specific for arsenate (Q_2 decreased slightly from 0.80 mmol g^{-1} to 0.74 mmol g^{-1}). The model shows that P was more competitive in occupying the low-binding-energy sites than that in the high-binding-energy sites for arsenate. When the molar ratio of As to P was 1:10, the Q value for arsenate was almost constant at 0.40 mmol g^{-1}, indicating that about 22% of the surface sites on the Fe–Ce absorbent would be exclusively specific for arsenate.

Generally speaking, the influence of F on arsenate adsorption was much weaker than that of P since the Fe–Ce retained a considerable adsorption capacity for arsenate even at an As/F ratio of 1:100. The Q, Q_1, and Q_2 values for arsenate were not markedly affected by the presence of F at an As/F ratio of 1:1. With decreasing the As/F ratio, the Q decreased, but not as significantly as in the case of the As/P systems (Table 1). Again, adsorption capacity of arsenate at the low-binding-energy sites was mainly affected by the presence of F, while that at the high-binding-energy sites only changed a little.

Considering the different competitive adsorption behaviors of P, F, and arsenate, it seems likely that there are some nonspecific sites on the Fe–Ce that are available for all three of the anions, while there are also some sites that are specific for each [12].

3.2. Mechanisms of competitive adsorption

3.2.1. Surface active sites for arsenate adsorption

It has been reported the hydrolysis reaction which takes place between the metal oxide and water results in the formation of surface hydroxyl groups. The surface hydroxyl groups on metal oxides are considered as the most abundant and active adsorption sites for adsorption of anions from water [28–30]. In our previous studies [6,7] the surface acidity and formation of surface hydroxyl groups of the Fe–Ce have been provide to the interpretation of the adsorption behaviors. At the same time, the exchange of surface sulfate groups has also been suggested to be an important mechanism for the removal of arsenate [31,32]. In the present study, sulfate was introduced in the Fe–Ce preparation process because of the use of Ce(SO$_4$)$_2$·4H$_2$O. In order to investigate if surface sulfate groups also play an important role in the adsorption process, the release of sulfate during arsenate adsorption was monitored at low (0.27–0.53 mM) and high (5.34–13.35 mM) initial As concentration (C_{0-As}) ranges, as shown in Fig. 2. On the basis of the slope of the regression line in Fig. 2, Fe–Ce releases 0.15 mmol and 0.24 mmol of SO$_4$ for every mmol of arsenate that has been sorbed at low and high C_{0-As} ranges, respectively. So sulfate might also be involved in the arsenate adsorption on Fe–Ce. In comparison with the result reported by Fukushi et al. [32] (schwertmannite released 0.62 mmol SO$_4^{2-}$ for every mmol of arsenate adsorbed), the relatively low release ratio shows that sulfate exchange was not the dominant mechanism for the adsorption of arsenate, and surface hydroxyl groups should be the major active sites.

3.2.2. XPS: proof of the existence of different surface active site types

The XPS analyses of the Fe–Ce absorbents were conducted before and after binding adsorption of arsenate, P, and F (Fig. 3 and Table 2). Significant decreases in the Fe(2p3) spectrum intensity were observed following arsenate and P adsorption (Fig. 3(a)), while the Ce(3d) spectra showed little change, suggesting the establishment of strong interactions between As/P and the active sites of Fe atoms. For the F adsorption system, on the other hand, the Fe(2p3) spectra only exhibited slight different before and after
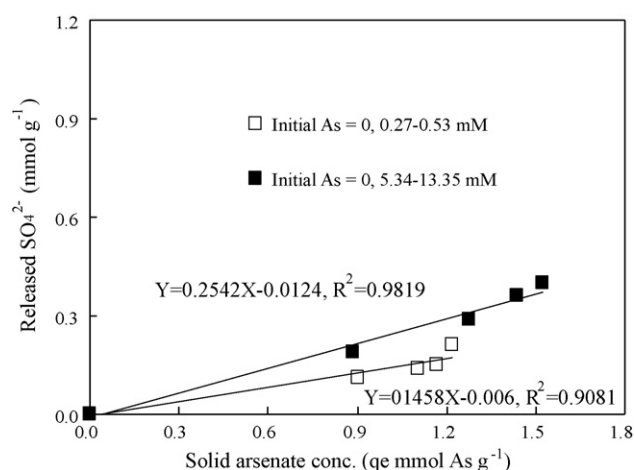
Fig. 2. Molar ratio of released sulfate to adsorbed solid-phase arsenate concentration at low (0.27–0.53 mM) and high (5.34–13.35 mM) initial As concentration ranges.

adsorption. However, the binding energy of Ce(3d5/2) decreased from 885.8 eV to 884.2 eV and the peak shape changed notably after F adsorption, suggesting the establishment of strong interactions between the F and the active sites of Ce atoms (Fig. 3(b)). Clearly,
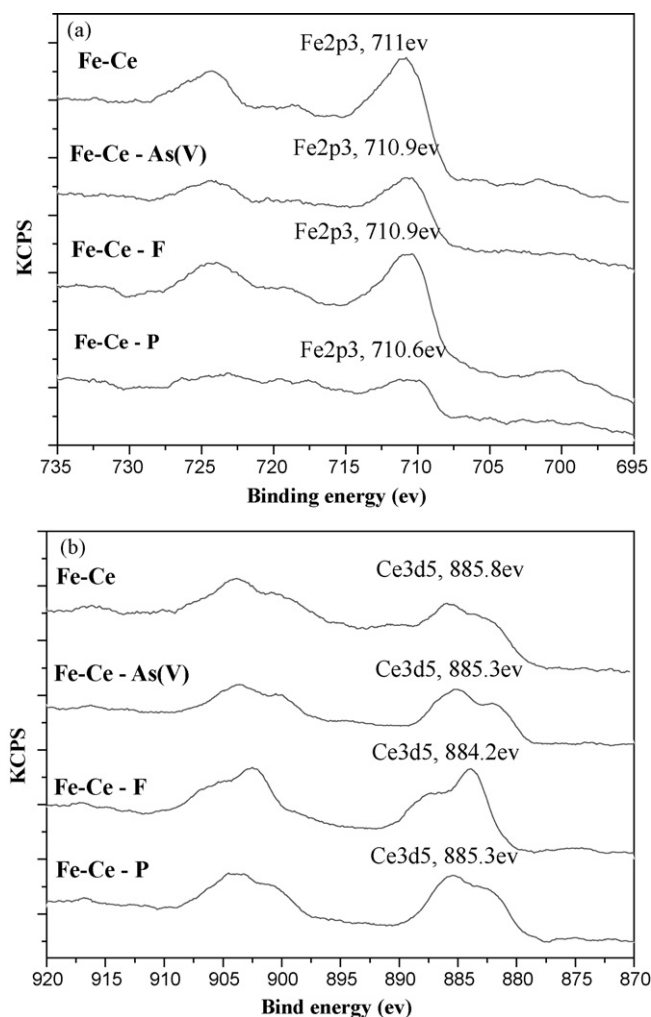
Fig. 3. XPS spectra for (a) Fe2p3 (b) Ce3d5, of the Fe–Ce adsorbent before and after arsenate, F, and P adsorption.

Table 2
Binding energies and atom percentages of surface elements collected from XPS of Fe–Ce before and after arsenate, P, and F adsorption.

Sample	Binding energy (eV)		Atom (%)			
	Fe2p3	Ce3d5	Fe	Ce	O	As/P/F
Fe–Ce	711.0	885.8	20.1	6.1	73.8	0
Fe–Ce–As	710.9	885.3	7.7	6.2	69.8	16.2
Fe–Ce–P	710.6	885.3	4.0	7.2	70.1	18.6
Fe–Ce–F	711.9	884.2	17.8	11.0	41.2	30.1

the Fe surface active group would appear to play a key role in arsenate and P adsorption, while the Ce surface active group appears to be important for the adsorption of F.

The relative amounts in terms of atom% of Ce, Fe, O and the target anions on the surface of Fe–Ce before and after anion adsorptions in different systems are summarized in Table 2. The Fe percentage on the Fe–Ce surface decreased drastically from 20.1% to 7.7% and 4.0%, respectively, after adsorption of arsenate and P, while that in the F adsorption system merely decreased to 17.8%. On the other hand, the Ce percentage, initially at 6.1%, remained almost unchanged fol-

lowing arsenate and P adsorption (6.2% and 7.2%, respectively), but increased to 11.0% following F adsorption. The changes in the Fe or Ce atom % were possibly attributed to the surface mask by different groups. The radii of arsenate and phosphate are 248 and 238 pm, respectively, much larger than that of surface hydroxyl (145 pm), while the F ion (133 pm) is smaller [29,33]. So the Fe percentage on the Fe–Ce surface decreased after adsorption of arsenate and P, while the Ce percentage increased following F adsorption.

3.2.3. EXAFS studies of Fe–Ce before and after As adsorption

EXAFS spectroscopy was employed to further determine the Fe (before adsorption) and As (after adsorption) local coordination environments. Fig. 4(a) and (b) shows the k^2 weighted observed (solid lines) along with model calculated (dot lines) Fe K-edge EXAFS spectra and the corresponding RSFs as Fourier transform (FT) versus radial distance for Fe–Ce sample before arsenate adsorption. The Fe K-edge XANES data are provided as the supporting material (Figure S2 and Table S3). Fig. 4(c) and (d) shows the k^3 weighted As K-edge EXAFS spectra and the RSFs for As adsorbed Fe–Ce and reference As compounds (CeAsO$_4$ and FeAsO$_4$·2H$_2$O). The resolved structure parameters obtained by fitting the theoretical paths to
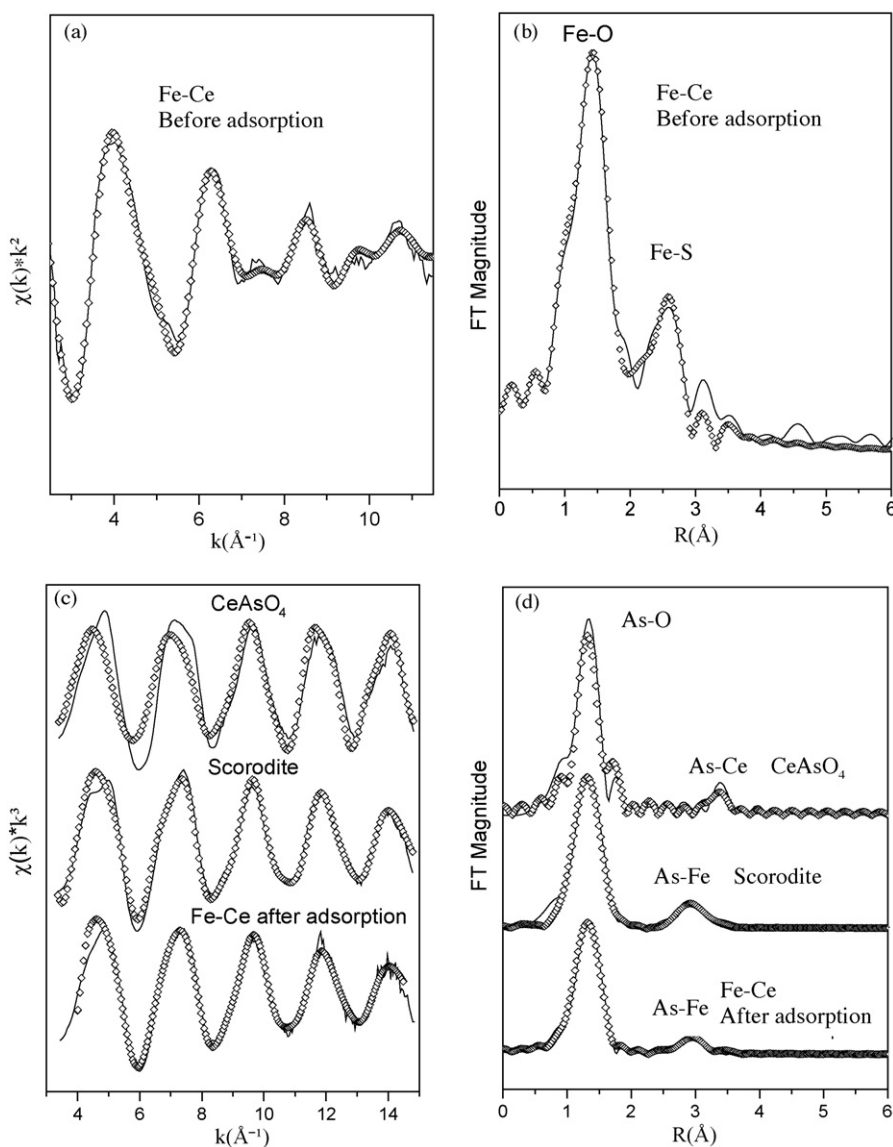

Fig. 4. The κ^3-weighted observed (solid line) and calculated (dotted line) Fe K-edge EXAFS spectra (a) and Fourier-transform magnitude (b) resulting in a radial distance structure for the Fe–Ce and the reference iron oxides. The peak positions are uncorrected for phase shift.

the experimental spectra are shown in the Supplementary material (Tables S1 and S2). The FT of the EXAFS spectra isolates the contributions of different coordination shells, in which the peak position corresponds to the interatomic distances. These peak positions in Fig. 4 are uncorrected for the phase shift, so they deviate from the true distance by 0.3–0.5 Å.

The Fe state in Fe–Ce was calculated from the correlation of Fe states and white line energy position in XANES spectra. The results show that the calculated Fe state was 2.45, indicated that Fe(II) and Fe(III) coexisted in Fe–Ce (Table S3).The first peak in the FT was the result of backscattering from the nearest neighbor Fe–O shell for Fe–Ce (Fig. 4(b)). The average Fe–O distance was about 1.95 Å, and the CN of oxygen was calculated to be 6.2. It was found that the best fit was obtained by using butlerite ($FeSO_7H_3$) [34] as reference model. So the second peak in the FT might be attributed to Fe–S bonding with an interatomic distance of 3.18 Å. Fitting the Fe–S peak was completed in both k-space and R-space using a Fe–S shell, resulting in a CN of 2.1. The results suggested that sulfate might have formed bidentate binuclear complexes with iron oxides. Combined with the sulfate leaching data in Fig. 2, it is estimated that sulfate groups on the surface possibly have also contributed to the adsorption of arsenate.

As shown in Fig. 4(d), the first peak in the FT was the result of backscattering from the nearest neighbor As–O shell for Fe–Ce after arsenate adsorption. The average As–O distance was 1.68 Å, which is in good agreement with previous publications [35–37]. The average CN of O was calculated to be 4.8. The second peak position in the FT, centered at about 2.99 Å (uncorrected for phase shift) which is in agreement with $FeAsO_4·2H_2O$ (As–Fe shell), but inconsistent with that of $CeAsO_4$ (As–Ce shell) as shown in Fig. 4(d). The fact that the second shell was As–Fe further supported the conclusion that arsenate adsorptions occur mainly at the Fe surface active sites rather than the Ce surface sites. The second peak could be fit with 2.3 Fe atoms at $R_{As–Fe}$ = 3.32 Å and 1.1 Fe atoms at $R_{As–Fe}$ = 3.55 Å from the central As atom, respectively (Table S2). Similar As–Fe distances at 3.32 Å (43–45) and 3.55 Å [38,39] were previously reported, respectively. The results suggested that bidentate binuclear and monodentate mononuclear inner-sphere complex species coexisted at the Fe–Ce surface, which corresponded to an As–Fe distance of 3.32 and 3.55 Å, respectively. Further information regarding the surface complexes will be provided in the next paper.

4. Conclusions

This study investigated the effects of F and P on arsenate removal as well as mechanisms involved using an Fe–Ce oxide adsorbent in this system. The following conclusions could be drawn from this study:

(1) The two-site adsorption isotherm revealed the presence of two kinds of adsorption sites (low- and high-binding-energy sites) with different binding affinities for arsenate. P strongly inhibited the adsorption of arsenate at the low-binding-energy sites. The coexistence of F, on the other hand, only influenced the total adsorption capacity of arsenate at high simultaneous F concentrations.
(2) Although surface hydroxyl groups should be the major active sites, the fact that Fe–Ce released 0.15–0.24 mmol sulfate for every mmol arsenate adsorbed and the second peak in the FT might be attributed to Fe–S bonding of the Fe K-edge EXAFS data, suggested that sulfate groups might have played a role for adsorption of arsenate.
(3) Arsenate and P are mainly adsorbed through the substitution of Fe surface active sites, while F is mainly adsorbed through

substitution of Ce surface active sites by XPS analyses on Fe–Ce surface. The As k-edge EXAFS data show that the second peak of Fe–Ce after arsenate adsorption is As–Fe shell, which further supported the above hypothesis that arsenate adsorption occurs mainly at the Fe surface active sites. The arsenate on the used Fe–Ce could be desorbed with an efficiency of 89% using 1.0 M sodium hydroxide, and the Fe–Ce after desorption showed similar arsenate adsorption performance with the fresh one. This part of the result will be reported in a future paper.

Appendix A. Supplementary data

Supplementary data associated with this article can be found, in the online version, at doi:10.1016/j.jhazmat.2010.02.081.

References

[1] USEPA, Technologies and Costs for Removal of Arsenic from Drinking Water, Report No. EPA-815-R-00-028, 2000.
[2] D. Mohan, C.U. Pittman Jr., Arsenic removal from water/wastewater using adsorbent—a critical review, J. Hazard. Mater. 142 (2007) 1–53.
[3] L.M. Del Razo, J.C. Corona, G. García-Vargas, A. Albores, M.E. Cebrián, Fluoride levels in well-water from a chronic arsenicism area of Northern Mexico, Environ. Pollut. 80 (1993) 91–94.
[4] P.L. Smedleya, M. Zhang, G. Zhang, Z. Luo, Mobilisation of arsenic and other trace elements in fluviolacustrine aquifers of the Huhhot Basin, Inner Mongolia, Appl. Geochem. 18 (2003) 1453–1477.
[5] D. Mohapatra, P. Singh, W. Zhang, P. Pullammanappallil, The effect of citrate, oxalate, acetate, silicate and phosphate on stability of synthetic arsenic-loaded ferrihydrite and Al-ferrihydrite, J. Hazard. Mater. 124 (2005) 95–100.
[6] Y. Zhang, M. Yang, X.M. Dou, H. He, D.S. Wang, Arsenate adsorption on an Fe–Ce bimetal oxide adsorbent: role of the surface properties, Environ. Sci. Technol. 39 (2005) 7246–7253.
[7] Y. Zhang, M. Yang, X. Huang, Arsenic(V) removal with a Ce(III)-doped iron oxide adsorbent, Chemosphere 51 (2003) 945–952.
[8] X.M. Dou, Y. Zhang, M. Yang, Y.S. Pei, X. Huang, T. Takayama, S. Kato, Occurrence of arsenic in groundwater in the suburbs of Beijing and its removal using an iron–cerium bimetal oxide adsorbent, Water Qual. Res. J. Can. 41 (2006) 140–146.
[9] R.L. Parfitt, Anion adsorption by soils and soil materials, Adv. Agron. 30 (1978) 1–50.
[10] P. Persson, N. Nilsson, S. Sjoberg, Structure and bonding of orthophosphate ions at the iron oxide–aqueous interface, J. Colloid Interf. Sci. 177 (1996) 263–275.
[11] H.S. Zhao, S. Robert, Competitive adsorption of phosphate and arsenate on goethite, Environ. Sci. Technol. 35 (2001) 4735–4757.
[12] F. Liu, A. De Cristofaro, A. Violante, Effect of pH, phosphate and oxalate on the adsorption/desorption of arsenate on/from goethite, Soil Sci. 166 (2001) 197–208.
[13] A. Violante, M. Pigna, Competitive sorption of arsenate and phosphate on different clay minerals and soils, Soil Sci. Soc. Am. J. 66 (2002) 1788–1796.
[14] B.A. Manning, S. Goldberg, Adsorption and stability of arsenic(III) at the clay mineral–water interface, Environ. Sci. Technol. 31 (1997) 2005–2011.
[15] J.K. Syers, M.G. Browman, G.W. Smillie, R.B. Corey, Phosphate sorption by soils evaluated by the Langmuir adsorption equation, Soil Sci. Soc. Am. Proc. 37 (1973) 358–363.
[16] I.C.R. Holford, R.W.M. Wedderburn, G.E.G. Mattingly, A Langmuir two-surface equation as a model for phosphate adsorption by soils, J. Soil Sci. 25 (1974) 242–255.
[17] I.C.R. Holford, G.E.G. Mattingly, A model for the behaviour of labile phosphate in soil, Plant Soil 44 (1976) 219–229.
[18] R. Melamed, J.J. Jurinak, L.M. Dudley, Effect of adsorbed phosphate on transport of arsenate through an oxisol, Soil Sci. Soc. Am. J. 60 (1995) 121–131.
[19] Y.B. Sui, M.L. Thompson, Phosphorus sorption, desorption, and buffering capacity in a biosolids-amended mollisol, Soil Sci. Soc. Am. J. 64 (2000) 164–169.
[20] W. Jiang, S.Z. Zhang, X.Q. Shan, M.H. Feng, Y.G. Zhu, R.G. McLaren, Adsorption of arsenate on soils. Part 1. Laboratory batch experiments using 16 Chinese soils with different physicochemical properties, Environ. Pollut. 138 (2005) 278–284.

[21] G. Karthikeyank, M.A. Tshabalala, D. Wang, M. Kalbasi, Solution chemistry effects on orthophosphate adsorption by cationized solid wood residues, Environ. Sci. Technol. 38 (2004) 904–911.

[22] X.M. Wu, Y. Zhang, X.M. Dou, M. Yang, Fluoride removal performance of a novel Fe-Al-Ce trimetal oxide adsorbent, Chemosphere 69 (2007) 1758–1764.

[23] F. Qin, B. Wen, X.Q. Shan, Y.N. Xie, T. Liu, S.Z. Zhang, S.U. Khan, Mechanism of competitive adsorption of Pb, Cu, Cd on peat, Environ. Pollut. 144 (2006) 669–680.

[24] U. Becker, M.F. Hochella Jr., J.V. David, The adsorption of gold to galena surfaces: Calculation of adsorption/reduction energies, reaction mechanism, XPS spectra, and STM images, Geochim. Cosmochim. Acta 61 (1997) 3565–3585.

[25] J.A. Mead, A comparison of the Langmuir, Freundlich and Temkin equations to describe phosphate adsorption properties of soils, Aust. J. Soil Res. 19 (1981) 333–342.

[26] T.J. Ressler, WinXAS: a program for X-ray absorption spectroscopy data analysis under MS-Windows, J. Synchrotron Radiat. 5 (1998) 118–122.

[27] A.L. Ankudinov, B. Ravel, J.J. Rehr, S.D. Conradson, Real space multiple-scattering calculation and interpretation of X-ray absorption near-edge structure, Phys. Rev. B 58 (1998) 7565–7576.

[28] T. Stumm, Chemistry of the Solid–Water Interface, John Wiley, New York, 1992.

[29] H. Tamura, K. Mita, A. Tanaka, M. Ito, Mechanism of hydroxylation of metal oxide surfaces, J. Colloid Interf. Sci. 243 (2001) 202–207.

[30] S. Tokunaga, M.J. Hardon, S.A. Wasay, Removal of fluoride ions from aqueous solution by multivalent metal compounds, Int. J. Environ. Stud. 48 (1995) 17–28.

[31] Y.F. Jia, G.D. Demopoulos, Adsorption of arsenate onto ferrihydrite from aqueous solution: influence of media (sulfate vs nitrate,), added gypsum, and pH alteration, Environ. Sci. Technol. 39 (2005) 9523–9527.

[32] K. Fukushi, T. Sato, N. Yanase, Solid-solution reactions in As(V) sorption by schwertmannite, Environ. Sci. Technol. 37 (2003) 3581–3586.

[33] A.G. Volkov, S. Cruz, Liquid–liquid Interfaces: Theory and Methods, CRC Press, Santa Cruz, CA, 1996.

[34] R.T. Downs, M. Hall-Wallace, The American mineralogist crystal structure database, American Mineralogist 88 (2003) 247–250.

[35] M. Pena, X.G. Meng, G.P. Korfiatia, C.Y. Jing, Adsorption mechanism of arsenic on nanocrystalline titanium dioxide, Environ. Sci. Technol. 40 (2006) 1257–1262.

[36] A.C.Q. Ladeira, V.S.T. Ciminelli, H.A. Duarte, M.C.M. Alves, A.Y. Ramos, Mechanism of anion retention from EXAFS and density functional calculations: arsenic(V) adsorbed on gibbsite, Geochim. Cosmochim. Acta 65 (2001) 1211–1217.

[37] C.Y. Jing, S.Q. Liu, R. Patel, X.G. Meng, Arsenic leachability in water treatment adsorbents, Environ. Sci. Technol. 39 (2005) 5481–5487.

[38] B.A. Manning, M.L. Hunt, C. Amarhein, J.A. Yarmoff, Arsenic(III) and arsinic(V) reactions with zerovalint iron corrosion products, Environ. Sci. Technol. 36 (2002) 5455–5461.

[39] S. Fendorf, M.J. Eick, P. Grossl, D.L. Sparks, Arsenate and chromate retention mechanisms on goethite. 1. Surface structure, Environ. Sci. Technol. 31 (1997) 315–319.